ICHEP'98 #204
Submitted to Pa 10
Pl 12

DELPHI 98-92 CONF 160
22 June, 1998

Search for Sfermions at $\sqrt{s} = 130$ to 183 GeV

Preliminary

DELPHI Collaboration

W. Adam [1], **P. Allport** [2], **S. Amato** [3], **M. Berggren** [4], **M. Besançon** [5], **A. Galloni** [2], **M. Gandelman** [3], **Ph. Gris** [5], **B. King** [2], **J.H. Lopes** [3], **N. Neumeister** [1], **R. Pain** [6], **Ph. Schwemling** [6]

Abstract

Data taken by the DELPHI experiment at centre-of-mass energy of 183 GeV has been used to search for the supersymmetric partners of electron, muon and tau leptons and of top and bottom quarks. The observations are in agreement with standard model predictions. These results were subsequently combined with those obtained by DELPHI during the 1995 and 1996 LEP runs and are interpreted in terms of exclusion regions in the ($M_{\tilde{f}}$, $M_{\tilde{\chi}_1^0}$) planes.

Paper submitted to the ICHEP'98 Conference
Vancouver, July 22-29

[1] Institut für Hochenergiephysik der ÖAW, Vienna, Austria
[2] University of Liverpool, England
[3] Univ. Federal do Rio de Janeiro, Brazil
[4] IPN, University Claude Bernard (Lyon I), Villeurbane, France
[5] CEA/DAPNIA/SPP, Saclay, France
[6] LPNHE, University of Paris VI & VII, Paris, France

1 Introduction

This paper reports on a search for scalar partners of leptons (sleptons) and quarks (squarks) in data taken by DELPHI in 1997 at a centre-of-mass energy, $\sqrt{s}$, of 183 GeV. Mass limits for these particles have already been published based on data taken at LEP2 [1], [2].

Scalar partners of right- and left-handed fermions are predicted by supersymmetric models and, in particular, by the minimal supersymmetric extension of the standard model (MSSM) [3]. They could be produced pairwise via e^+e^- annihilation into Z^0/γ. Selectron production could be enhanced by a contribution from t-channel neutralino exchange, which introduces a direct dependence on the neutralino parameters and the possibility of $\tilde{e}_L$,$\tilde{e}_R$ final states even without mixing via the mass matrix. Important effects caused by off-diagonal terms in the mass matrix are only predicted for the partner of heavy fermions, i.e. for top and bottom quarks (stop and sbottom) and for tau leptons (stau). As a consequence their lighter states are candidates for the lightest charged supersymmetric particle.

Throughout this paper conservation of R-parity is assumed, which implies that the lightest supersymmetric particle (LSP) is stable. In this paper the LSP is assumed to be either the lightest neutralino, $\tilde{\chi}^0_1$, or a sneutrino, $\tilde{\nu}$. These particles only weakly interact with normal matter, such that events will be characterised by missing momentum and energy.

In a large fraction of MSSM parameter space sfermions are supposed to decay dominantly into the corresponding fermion and the lightest neutralino. Consequently only these decay modes were considered for all analyses presented in this paper, with the exception of the search for stop squarks. In this case the standard decay channel is kinematically not allowed, and a stop decay into a bottom quark and a chargino is disfavoured in view of existing limits on the chargino mass [4]. The dominant two-body decay channel is thus the one into a charm quark and a neutralino.

If, however, a sufficiently light sneutrino exists, the three-body decay $\tilde{t} \to b\ell\tilde{\nu}$, which proceeds via a virtual chargino, could occur. The branching fractions into the different lepton flavours are determined by the character of the intermediate chargino. If it is mainly the supersymmetric partner of the W ("wino-like") the branching fractions are about equal. If it is on the contrary "higgsino-like" the decay into $b\tau\tilde{\nu}_\tau$ is considerably enhanced. A special analysis was designed to search for these three-body decay modes. The mirror decay channel into $b\nu\tilde{\ell}$ is unlikely to be open in view of the mass limits for sleptons and is not considered in this paper.

2 Detector description

The DELPHI detector and its performance have been described in detail elsewhere [5, 6]; only those components relevant for the present analyses are discussed here. Charged particle tracks were reconstructed in the 1.2 T solenoidal magnetic field by a system of cylindrical tracking chambers. These were the Microvertex Detector (VD), the Inner Detector (ID), the Time Projection Chamber (TPC) and the Outer Detector (OD). In addition, two planes of drift chambers aligned perpendicular to the beam axis (Forward Chambers A and B) tracked particles in the forward and backward directions, covering

polar angles $11^\circ < \theta < 33^\circ$ and $147^\circ < \theta < 169^\circ$ with respect to the beam (z) direction.

The VD consisted of three cylindrical layers of silicon detectors, at radii 6.3 cm, 9.0 cm and 11.0 cm. All three layers measured coordinates in the plane transverse to the beam. The closest (6.3 cm) and the outer (11.0 cm) layers contained double-sided detectors to also measure z coordinates. In 1996 the polar angle coverage of the VD was from 24° to 156° and detectors were added to the inner layer providing a measurement of the z coordinate. The ID was a cylindrical drift chamber (inner radius 12 cm and outer radius 22 cm) covering polar angles between 15° and 165°. The TPC, the principal tracking device of DELPHI, was a cylinder of 30 cm inner radius, 122 cm outer radius and had a length of 2.7 m. Each end-plate was divided into 6 sectors, with 192 sense wires used for the dE/dx measurement and 16 circular pad rows used for 3 dimensional space-point reconstruction. The OD consisted of 5 layers of drift cells at radii between 192 cm and 208 cm, covering polar angles between 43° and 137°.

The average momentum resolution for the charged particles in hadronic final states was in the range $\Delta p/p^2 \simeq 0.001$ to $0.01(\mathrm{GeV}/c)^{-1}$, depending on which detectors were used in the track fit [6].

The electromagnetic calorimeters were the High density Projection Chamber (HPC) covering the barrel region of $40^\circ < \theta < 140^\circ$, the Forward ElectroMagnetic Calorimeter (FEMC) covering $11^\circ < \theta < 36^\circ$ and $144^\circ < \theta < 169^\circ$, and the STIC, a Scintillator TIle Calorimeter which extended coverage down to 1.66° from the beam axis in both directions. The 40° taggers were a series of single layer scintillator-lead counters used to veto electromagnetic particles that would otherwise have been missed in the region between the HPC and FEMC. The efficiency to register a photon with energy above 5 GeV at polar angles between 20° and 160°, measured with the LEP1 data, was above 99% [7]. The hadron calorimeter (HCAL) covered 98% of the solid angle. Muons with momenta above 2 GeV/c penetrated the HCAL and were recorded in a set of Muon Drift Chambers.

Muon identification was provided primarily by the algorithm described in [6] which relies on the association of charged particle tracks to signals in the barrel and forward muon chambers. The same algorithm has been also extended to the surrounding muons chambers. The longitudinal profile of the energy deposit in the hadron calorimeter was also used to improve efficiency of the muon identification. Electrons were identified as charged particle tracks with an energy deposit above 3 GeV in the electromagnetic calorimeter, below 1.6 GeV beyond the first layer of the hadronic calorimeter and with a ratio of the electromagnetic calorimeter energy to the momentum from tracking above 0.3.

Decays of b-quarks were tagged using a probabilistic method based on the impact parameters of tracks with respect to the main vertex. The quantity $\mathcal{P}_E$ was the probability that all tracks were compatible with the main vertex. $\mathcal{P}_E^+$ was the corresponding probability for tracks with positive impact parameters, the sign of the impact parameter being defined by the jet direction. The combined probability $\mathcal{P}_{comb}$ included in addition contributions from properties of reconstructed secondary vertices [8].

3 Data samples, event generators and limits

Data were taken during the 1997 LEP run at a mean centre-of-mass energy of 183 GeV, corresponding to an integrated luminosity of 53 pb^{-1}.

Simulated events were generated with several different programs in order to evaluate signal efficiency and background contamination. All the models used JETSET 7.4 [9] for quark fragmentation with parameters tuned to represent DELPHI data [10].

The program SUSYGEN [11] was used to generate slepton events and to calculate cross-sections and branching ratios. It was verified that the result obtained agreed with the calculations of reference [12]. Stop and sbottom events were generated according to the expected differential cross-sections, using the BASES and SPRING program packages [13]. Special care was taken in the modelling of the stop hadronisation [14].

The background processes $e^+e^- \to q\bar{q}(n\gamma)$ and processes leading to four-fermion final states, $(Z^0/\gamma)^*(Z^0/\gamma)^*$, $W^{+*}W^{-*}$, $We\nu_e$, and $Z^0e^+e^-$ were generated using PYTHIA [9]. The cut on the invariant mass of the virtual $(Z^0/\gamma)^*$ in the $(Z^0/\gamma)^*(Z^0/\gamma)^*$ process was set at 2 GeV/c^2, in order to determine the background from low mass ff pairs. The calculation of the four-fermion background was verified using the program EXCALIBUR [15], which consistently takes into account all amplitudes leading to a given four-fermion final state. The version of EXCALIBUR used did not, however, include the transverse momentum of initial state radiation. Two-photon interactions leading to hadronic final states were simulated using TWOGAM [16] and BDKRC [17] for the Quark Parton Model contribution. Leptonic final states with muons and taus were also modelled with BDKRC. BDK [17] was used for final states with electrons only.

Generated signal and background events were passed through detailed detector response simulation [18] and processed with the same reconstruction and analysis programs as the real data. The number of background events simulated was mostly several times larger than the number expected in the real data.

The likelihood ratio method described in [19] was used for the calculation of exclusion zones, combining the results from different centre-of-mass energies. It provides an optimal combination for each mass taking into account the expected levels of background and signal and the number of candidates. Expected exclusion zones were calculated using the same algorithm, from simulated background-only experiments.

4 Search for selectrons and smuons

4.1 Selection of selectrons

To search for selectrons, the general topology required was acoplanar electrons and missing momentum. The selection was optimised both on simulated background and signal events to reduce the expected Standard Model background, while keeping a reasonable efficiency for the signal over a wide range of $M_{\tilde{e}} - M_{\tilde{\chi}^0_1}$ combinations.

The first stage of the event selection kept all candidates with exactly two well reconstructed charged particles of opposite charge with momentum above 1 GeV/c. In addition, to reduce two-photon backgrounds, the invariant mass of the two particle system was required to be greater than 4.5 GeV/c^2.

Both particles were also required to have no associated muon chamber or hadron calorimeter hits and at least one of the two charged particles was required to be loosely identified as an electron. The agreement between the data and Monte Carlo samples before further selections is illustrated by the first two plots of Figure 1.

Constraints on the visible energy (15 GeV $< E_{vis} <$ 100 GeV) were then imposed to

further reduce two-photon backgrounds and conventional high energy e^+e^- annihilation processes. The unassociated neutral energy (outside a 10° cone around the track) in the event was required to be less than 30 GeV and it was demanded that there were less than four neutral clusters in total with an $E_{min} > 0.5$ GeV.

To further reduce two-photon backgrounds, the energy measured in the STIC was required to be less than 4 GeV. The momentum of each track was demanded to be between 2 and 100 GeV/c. It was further required that the missing momentum vector pointed towards active components of the DELPHI detector.

Collinear events were rejected if the opening angle between the tracks was greater than 165°, corresponding to an acollinearity $\phi_{acol} < 15°$, and a cut on the acoplanarity was imposed at $\phi_{acop} > 15°$, corresponding to an opening angle in the $R\phi$ plane smaller than 165°. Finally a lower cut at 5 GeV/c was made on the transverse momentum of the pair of particles.

The efficiencies have been determined for each point of a 1 GeV × 1 GeV grid in the ($M_{\tilde{e}}$,$M_{\tilde{\chi}^0_1}$) plane, using a fast detector simulation. The results have been verified for a subset of points using the full detector simulation.

11 candidates were found, using the above selections, where a background of 12.7±0.8 was expected. Table 1 shows the contributions to the total background. Efficiencies, obtained from simulated signal Monte Carlo events, are plotted in Figure 2.

4.2 Selection of smuons

The topology searched for was two acoplanar muons and missing momentum. The selection criteria were based on the need to keep signal sensitivity as high as possible for a wide range of $M_{\tilde{\mu}} - M_{\tilde{\chi}^0_1}$ combinations, while at the same time rejecting as much of the expected backgrounds as feasible.

To select the di-muon topology, exactly two well reconstructed oppositely charged particles with momenta above 1 GeV/c were required. In addition, to reduce two-photon backgrounds, the invariant mass of the two particle system was required to be greater than 4.5 GeV/c^2.

Both particles were further required to have hits in at least 2 of the outer 3 layers of the Hadron Calorimeter and not to be identified as electrons. At least one of the two charged particles was required to be loosely identified as a muon. The agreement between the data and Monte Carlo samples is illustrated by the last two plots of Figure 1.

Constraints on the visible energy (10 GeV $< E_{vis} <$ 120 GeV) were then imposed to further reduce two-photon backgrounds and conventional high energy e^+e^- annihilation processes. For the same reason, the total energy contained in the STIC was required to be less than 1 GeV. The number of unassociated neutral clusters was then required to be less than two (using the same definitions as for the selectron analysis).

Smuons, unlike selectrons, cannot be produced via $t-$channel processes. This means that their production cross-section should be less and the direction of the decay μ^- (μ^+) should be uncorrelated with the direction of the incoming e^- (e^+). Since the principle remaining background ($W-$ production) is strongly forward peaked, a cut on $q \times \cos\theta$ of $< 120°$, where q is the charge of the muon, is used to preferentially reduces this background.

It was demanded that the leading track momentum was above 5 GeV/c with the second track above 4 GeV/c and neither measured to be greater than 100 GeV/c. Cuts

on the acollinearity ($> 15°$), acoplanarity ($> 15°$) and the transverse momentum of the pair of tracks (> 5 GeV/c) were also applied. Finally, it was required that the missing momentum vector pointed towards active components of the DELPHI detector.

The efficiencies have been determined for each point of a 1 GeV $\times$ 1 GeV grid in the ($M_{\tilde{\mu}}$,$M_{\tilde{\chi}^0_1}$) plane, using a fast detector simulation. The results have been verified for a subset of points using the full detector simulation.

5 candidates were found where a background of 6.1$\pm$0.6 was expected. Table 2 summarises the number of accepted events in the data, together with the predicted number of events from standard model background sources. The efficiencies, obtained from simulated signal Monte Carlo events, are plotted in Figure 3.

5 Search for staus

5.1 Search for heavy staus

To select events with a signature of two acoplanar taus with high missing energy, a set of selection criteria was established. Well reconstructed charged and neutral particles were grouped together. To start with, charged tracks were merged if their invariant mass was below 5.5 GeV/c^2; if more than one such grouping was possible, the one with the lowest mass was retained. This procedure was repeated until no more low-mass merged groups could be constructed. Once the procedure was completed, neutrals were associated to the groups, as long as the invariant mass of the group with the neutral included did not exceed 5.5 GeV/c^2. Neutrals that could not be associated to any group were defined to be isolated neutrals. Comparison between data and simulation, after selection into two such groupings of particles, showed very good agreement, as can be seen in Figure 4.

Events with exactly two particle groups were considered further if

- the acoplanarity was between 4° and 169°,
- there was no calorimetric energy in a 30° cone around the beam-axis,
- the total number of reconstructed tracks was six or less,
- the energy of the most energetic, isolated photon was below 20 GeV,
- there were at least two tracks with momenta above 1 GeV/c and at an angle of more than 30° to the beam in the event, and at least one with momentum above 5 GeV/c,
- the absolute value of the total charge of the event was less than two,
- no signal in the 40° taggers isolated from any reconstructed particle was seen.

This selection was supplemented by cuts that depended on the point in the ($M_{\tilde{\tau}}$,$M_{\tilde{\chi}^0_1}$) plane considered:

- If the difference between the masses, ΔM, was above 50 GeV/c^2, then the square of transverse momentum with respect to the thrust axis, δ, was required to be greater than 0.4 (GeV/c)^2;
- if it was between 50 GeV/c^2 and 22 GeV/c^2 ; δ was required to be above 1 (GeV/c)^2, and the invariant mass of the visible system was required to be below 60 GeV/c^2;
- if it was below 22 GeV/c^2, the invariant mass was also required to be below 60 GeV/$c^2$and δ had to be above 0.4 (GeV/c)^2.

The events passing these cuts were then classified in four categories, according to the background channel mostly contributing, using the momentum of the most energetic charged particle in the event, p^{ch}_{max}, and the acoplanarity:

- Events with $p^{ch}_{max} \leq 10$ GeV/c, irrespective of the acoplanarity, were classified as "$\gamma\gamma$"-like. The background in this class was reduced by removing events with low missing transverse momentum. The value of the cut depended on the mass-point considered: 5.5, 6, and 9 GeV/c ; for mass differences less than 22 GeV/c^2, from 22 to 50 GeV/$c^2$and greater than 50 GeV/c^2, respectively. In addition it was demanded that the missing momentum should be above $(14^\circ - 0.2\theta_{acop})$(GeV/$c$)/$^\circ$. The latter condition removed events that simultaneously had low acoplanarity and transverse momentum, which is typical of two-photon events.
- Events with a 10 GeV/c $< p^{ch}_{max} \leq 60$ GeV/c and an acoplanarity $\leq 15^\circ$ entered in the "$Z^0/\gamma \to \tau^+\tau^-$" class. The background in this class was reduced by demanding that the vector sum of the momenta was at an angle of more than 30° to the beam.
- The same momentum range as above, but with an acoplanarity above 15°, defined the "WW" class. In this class the background tends to have larger momenta than the signal. While a W-boson decaying into a tau and a neutrino is indistinguishable from a stau decaying into a tau and a low-mass neutralino, the two Ws need not decay into the same final state. Hence, it was demanded that the momentum of the most energetic lepton in the event was less than 30 GeV/c. Since WW events show a large forward-backward asymmetry, contrary to the case of the signal, it was also demanded that, treating the event as W^+W^- pair production, the reconstructed polar angle of the W^+ be lower than 143° from the direction of the incident e^--beam. This class of events also contains a sizable background from radiative return and $\gamma\gamma$ events with an ISR photon. To reduce these sources, it was also required that the vector sum of the momenta was at an angle above 30° to the beam.
- Finally events with $p^{ch}_{max} > 60$ GeV/c were classified as "$Z^0/\gamma \to \mu^+\mu^-$"-like. However, for the masses interesting for this analysis the cross section for this class is so low that it was not considered further.

Table 3 summarises the number of accepted events in the data for the different selections together with the expected numbers of events from the different background channels. 7 candidates were found, at an expected background of 7.5±0.6 . The efficiencies have been determined using 5000 events for each point of a 1 GeV/c^2 × 1 GeV/c^2 grid in the ($M_{\tilde{\tau}}$,$M_{\tilde{\chi}^0_1}$) plane, using a fast detector simulation. The results have been verified with the full detector simulation and analysis chain and are shown in Figure 5.

5.2 Search for light staus without coupling to the Z^0

The analysis described above was effective for stau masses above about 25 GeV/c^2. Below that limit the efficiency rapidly dropped, mainly because the stau decay products tend to be back-to-back and fail to pass the acoplanarity cut. To a large extent light staus can be excluded using the agreement of the width of the Z^0-resonance with the standard model prediction, as observed at LEP1 [21]. The corresponding cross section limit of 150 pb for non-standard processes at $\sqrt{s} = M_Z$ excludes a $\tilde{\tau}_R$ below 25 GeV/c^2. However, at the stau mixing angle equivalent to the minimum cross section, the coupling to the Z^0 vanishes and no exclusion is possible using the width of the Z^0.

Therefore a specific search for staus with masses in the range from 1.8 to 26.5 GeV/c^2 and a mixing angle corresponding to the minimum cross section was designed. Relaxing the cut on acoplanarity resulted in higher backgrounds, which could be accepted due to the higher cross sections at these stau masses.

Two different sets of cuts were used: one for very low masses ($M_{\tilde{\tau}} < 6.5$ GeV/c^2) and one for fairly low masses (6.5 GeV/c^2 $< M_{\tilde{\tau}} <$ 26.5 GeV/c^2). Compared to the cuts described in section 5.1, the following changes were applied in both cases and for all background classes: No isolated photon was accepted, the second largest impact parameter in the transverse plane ($R\phi$) was required to be smaller than 1 mm in order to remove cosmics, and δ had to be above 7×10^{-4} (GeV/c)^2.

In the "$\gamma\gamma$" class a missing transverse momentum of at least 6.4 GeV/c was demanded and the cut as a function of $\theta_{\rm acop}$ was removed. In the "$Z^0/\gamma \to \tau^+\tau^-$" class, events with an effective centre-of-mass energy, $\sqrt{s'}$ [20], between 73.5 and 110.5 GeV were removed. In the "WW" class, the momentum of the stau candidates had to be below 57 GeV/c, and a lepton momentum below 26 GeV/c was required. For the "$Z^0/\gamma \to \tau^+\tau^-$" and the "WW" classes the vector sum of the momenta had to be more than 40° from the beam axis.

In the very low mass case, the cut on the maximum jet momentum was relaxed to 80 GeV/c, and the acoplanarity had to be in the range 0.05 to 26 degrees. In the low mass case, a more restrictive cut on the acoplanarity was used: $1.5° < \phi_{acop} < 26°$.

73 events passed the very low mass cuts, while 12 passed the fairly low mass cuts. The corresponding expected backgrounds were 77.5 and 14.8 events, respectively. The efficiencies were practically flat for both mass ranges. In the very low mass case, the efficiency was around 40% for all $\Delta M > M_\tau$ (1.8 GeV/c^2). In the low mass case it was around 30%, decreasing for $\Delta M < 4$ GeV/c^2.

6 Search for two-body decays of stop and sbottom

In this section a search for stop and sbottom in the decay modes $c\tilde{\chi}^0_1$ and $b\tilde{\chi}^0_1$, respectively, is presented. In both cases the experimental signatures consist of events with two jets and missing momentum. Since event parameters, such as visible energy, depend highly on the mass difference ΔM between squark and LSP, optimised selection procedures were used for the degenerate ($\Delta M \leq 10$ GeV/c^2), and the non-degenerate ($\Delta M > 10$ GeV/c^2) mass case. The main differences between stop and sbottom events arise from the hadronisation, which occurs either before ($\tilde{\rm t}$) or after ($\tilde{\rm b}$) the decay of the scalar quark. These differences are visible in particular in the degenerate mass case. Consequently different selections were used for the stop and sbottom analyses in the degenerate mass case whereas the selections were identical in the non-degenerate mass case.

In a first step particles were selected and clustered into jets. Reconstructed charged particles were required to have momenta above 100 MeV/c and impact parameters below 4 cm in the transverse plane and below 10 cm in the beam direction. Clusters in the calorimeters were interpreted as neutral particles if they were not associated to charged particles, and if their energy exceeded 100 MeV. Jets were reconstructed using the Durham algorithm with the critical distance set to 0.08.

In the second step of the analysis hadronic events were selected. Only two-jet events were accepted. The following requirements were optimised separately for the two ΔM

regions:

Non-degenerate mass case: For both the stop and sbottom analysis hadronic events were selected by requiring at least eight charged particles, a total transverse energy greater than 15 GeV and a transverse energy of the most energetic jet greater than 10 GeV. These three cuts were also aimed at reducing the background coming from two-photon processes. Forward Bhabha scattering was suppressed by requiring that the total energy in the FEMC was lower than 25 GeV. Z(γ) processes with a detected photon were reduced by requiring that the total energy in the HPC was lower than 40 GeV. Finally substantial missing energy was asked for by demanding that the effective centre-of-mass energy was lower than 170 GeV.

Degenerate mass case: For the selection of hadronic events for the stop analysis the number of charged particles was required to be greater than five, the total charged energy had to be lower than $0.3\sqrt{s}$ in order to select events with missing energy and the polar angle of the total missing momentum had to be in the interval $[15°, 165°]$, off the forward region, in order to reduce the background from radiative return events. The total energy in the FEMC and HPC had to be lower than 10 GeV and 40 GeV, respectively. The reduction of two-photon processes was ensured by requiring that the total transverse energy was greater than 5 GeV and that the quantity $p_{tt} = \sqrt{p_{tt1}^2 + p_{tt2}^2}$ was greater than 5 GeV, where p_{tti} was the transverse momentum of jet i with respect to the thrust axis in the transverse plane. Finally, the most energetic charged particle was required to have a polar angle in the interval $[30°, 150°]$ and a momentum greater than 2 GeV/c. Similarly the polar angle of the most energetic neutral particle was required to be in the interval $[20°, 160°]$. For the sbottom analysis only the cut on p_{tt} has been replaced by the requirement $p_{tt}/E_{vis} > 0.5$.

In a third step discriminating linear functions [22] were used to achieve optimum rejection power. The composition of the functions is shown in Table 4. They have been determined in the following way:

Non-degenerate mass case: In this case, the same functions have been used both for the stop and the sbottom analysis. A first discriminating linear function has been determined using training samples of signal and Z(γ) background processes. For the training of a second discriminating linear function signal and WW background event samples have been used. In the non-degenerate mass case, these two sources of background processes were found to be dominant after the first and second step of the event selection.

Degenerate mass case: Here the main source of background remaining after the first and second step of the event selection was found to be $\gamma\gamma$ events. Different functions have been determined for the stop and sbottom analyses using training samples of signal and two-photon events.

The final background reduction was performed by sequential cuts. In the non-degenerate mass case, one set of cuts was used to select both stop and sbottom events. It is shown, together with the number of events retained in data and background simulation, in Table 5. In the degenerate case two different selections were used for stop and sbottom, shown in Tables 6 and 7. The distributions of the discriminating functions for data and for background and signal Monte Carlo are shown in Figure 6.

The number of candidates found and the expected background levels are shown in Table 8. The efficiencies of the stop and sbottom signal selection are summarised in Figure 7. They have been evaluated using 35 simulated samples at different points in the ($M_{\tilde{\mathrm{q}}}$,$M_{\tilde{\chi}^0_1}$) plane, for squark masses between 50 and 90 GeV/c^2 and neutralino masses between 0 and 85 GeV/c^2.

7 Search for stop decays into $\mathrm{b}\ell\tilde{\nu}$

The experimental signature for $\mathrm{e^+e^-} \to \tilde{\mathrm{t}}\bar{\tilde{\mathrm{t}}}$ events, where the stop quarks decay into $\mathrm{b}\ell\tilde{\nu}$, is two acoplanar b-jets accompanied by two leptons and missing transverse momentum. As already mentioned in section 6 the event topology strongly depends on ΔM, the mass difference between the stop and the sneutrino. For small ΔM the transverse momentum carried by the sneutrino is small with respect to the original stop momentum. Also the energy available for the visible system is small and the events are very similar to $\gamma\gamma \to \mathrm{q\bar{q}}$ events, characterised by low visible mass, M_{vis}, low missing transverse momentum, p_T^{miss}, and a large fraction of the event energy in the very forward direction. If ΔM is large, a considerable amount of energy is available for the visible system and the events resemble those from WW, ZZ or $\mathrm{q\bar{q}}$ processes.

In the selection process a first set of cuts was applied in order to enrich the sample in hadronic events with missing momentum and to reject events concentrated in the very forward/backward regions:

- The number of charged particles, N^{ch}, had to be greater than 5,
- the ratio of "good" tracks to the total number of reconstructed tracks was required to be greater than 0.4, where "good" tracks were those with at least four measured points in the TPC, a polar angle in the interval [25°,155°] and $\delta p/p < 0.5$,
- the scalar transverse energy, $\sum \sqrt{p_T^2 + M^2}$, had to be greater than 10 GeV,
- the missing transverse momentum greater than 3.5 GeV/c,
- the missing momentum vector had to be in the polar angle range defined by $|\cos\theta(\mathbf{p}^{miss})| < 0.90$,
- less than 70% of the visible energy were allowed in a 30° cone around the beam axis,
- the charged energy was required to be greater than 6 GeV,
- the polar angle of the thrust axis was restricted by the condition $|\cos\theta_{thr}| < 0.98$.

At this stage 3212 events were left in the data sample, compared to 3193 events in the Monte Carlo sample.

In a second step the candidate events were selected. The visible mass had to be in the range 5–70 GeV. The event thrust had to satisfy $0.58 < \mathrm{Thrust} < 0.95$, and $E_{vis}/\sqrt{s}$ was required to be smaller than 0.4. At least one reconstructed electron or muon with a momentum greater than 1 GeV/c, or at least one tau was required. Tau candidates were selected using the Durham clustering algorithm with y_{cut} set to 0.004. A reconstructed jet was identified as tau if it contained only one or three charged particles, if the invariant mass of the jet was smaller than 2 GeV/c^2, if its neutral energy was greater than 0.4 GeV, its total energy was less than 40 GeV and if the angle to the nearest jet was larger than 19.5°. The jet multiplicity at this value of y_{cut} was required to be greater than three. The acoplanarity of the event was measured by forcing the event into a two-jet topology

using the Durham algorithm. The polar angles of both jets where required to satisfy $|\cos\theta_{jet}| < 0.93$. The acoplanarity was required to be greater than 14.9°. Finally the events were required to be b-tagged by asking for $\log_{10}(\mathcal{P}_E) > -0.48$.

The number of selected events after each of the two steps of the selection is shown in Table 9 for data and Monte Carlo. 3 candidates where found at an expected background of 3.4 events. The efficiency of the selection was computed using a sample of simulated signal events. Both the case of equal branching fraction into each lepton flavour and of a 100% branching fraction into tau leptons was considered. 1000 events were generated for each case at 30 points in the ($M_{\tilde{\mathrm{t}}}$, $M_{\tilde{\nu}}$) plane and passed through the full detector simulation and reconstruction programs. The efficiencies are shown in Figures 8 and 9. In general the efficiencies were at the 40% level, except for the region of mass differences between the stop and the sneutrino smaller than 10 GeV/c^2, were they dropped to a few percent.

8 Results

Limits on sfermion masses can be derived using several different assumptions. Scalar mass unification suggests lower masses and cross sections for the partners of right handed fermions. Hence these cross sections have been used to set conservative mass limits for selectrons and smuons, assuming the left handed state to be kinematically inaccessible. The branching ratios into $\ell\tilde{\chi}_1^0$ have been calculated with the supersymmetry conserving mass parameter, μ, set to -100 GeV/c^2, and the ratio of the vacuum expectation values of the two Higgs doublets, $\tan\beta$, set to 1.5 .

For the stau sleptons as well as for stop and sbottom squarks, which can be subject to substantial mass splitting via the mass matrix, limits for the state with minimal cross section have been calculated. A 100% branching ratio has been assumed for the decay channels analysed: $\tilde{\tau} \to \tau\tilde{\chi}_1^0$, $\tilde{\mathrm{t}} \to \mathrm{c}\tilde{\chi}_1^0$ and $\tilde{\mathrm{t}} \to \mathrm{b}\ell\tilde{\nu}$, and $\tilde{\mathrm{b}} \to \mathrm{b}\tilde{\chi}_1^0$.

In the calculation of the limits the results of the searches presented in this paper have been combined with those obtained by DELPHI from previous data sets.

8.1 Exclusion limits for selectrons and smuons

In the calculation of limits for selectron and smuon masses the kinematically allowed region for the momentum of the final state leptons has been used, taking into account candidates and background simulation events only in those regions of the ($\tilde{\ell}$,$M_{\tilde{\chi}_1^0}$) mass plane where they were valid.

Exclusion limits on $\tilde{\mathrm{e}}_R\tilde{\mathrm{e}}_R$ production were calculated for the MSSM parameters $\mu = -100$ GeV/c^2 and $\tan\beta = 1.5$. The same parameters were used to derive limits on the $\tilde{\mu}_R$ and $\tilde{\tau}_R$ masses, but in this cases thes dependence on these parameters is only weak, due to the absence of a t-channel diagram. Figures 10a and 10b show the 95% confidence level exclusion regions in the ($M_{\tilde{\ell}}$,$M_{\tilde{\chi}_1^0}$) plane.

8.2 Exclusion limits for staus

Unlike for selectrons and smuons there is no lower limit on the visible momentum of stau decay products. Hence, all candidates found both in data and in the simulated background

had to be taken into account for all points in the mass plane with $p^{max}_{seen} < p^{max}_{theor}(M_{\tilde{\tau}}, M_{\tilde{\chi}^0_1})$. Combining the efficiency, the background level and the number of candidates at each point in the $(\tilde{\tau},\tilde{\chi}^0_1)$ mass plane yielded the 95% confidence level exclusion regions for $\tilde{\tau}_R$ (Figure 10c). For this mixing angle the low mass region has already been excluded by the LEP1 measurement of the Z^0 resonance width. For the state with minimum cross section, however, low masses cannot be excluded in this way, and the results of the dedicated analysis were used for $M_{\tilde{\tau}} < 26.5\,\mathrm{GeV}/c^2$ (Figure 10d).

8.3 Exclusion limits for stop and sbottom

No evidence for stop or sbottom production has been found, neither in the two-body decay channels, nor in the three-body decay channel of the stop.

Figure 11 shows the $(M_{\tilde{q}},M_{\tilde{\chi}^0_1})$ regions excluded at 95% confidence level by the search for $\tilde{t} \to c\tilde{\chi}^0_1$ (a) and $\tilde{b} \to b\tilde{\chi}^0_1$ (b) decays, both for purely left-handed states and the states with minimum cross section.

The search for the three-body decay $\tilde{t} \to b\ell\tilde{\nu}$ yielded the exclusion regions shown in Figure 11 under the assumptions of equal branching fractions for the three lepton flavours (c) and of exclusive decays to the tau channel (d).

9 Conclusions

In a data sample of 53 pb^{-1} collected by the DELPHI detector at a centre-of-mass energy of 183 GeV, searches were performed for events with acoplanar lepton or jet pairs, or acoplanar jet pairs with two accompanying leptons. The results were combined with those already obtained between 130–172 GeV .

11 candidates were found in the selectron channel, in agreement with the background expectation. For $\mu = -100\,\mathrm{GeV}/c^2$ and for $\tan\beta = 1.5$, a mass limit for $\tilde{e}_R$ can be set at 81.4 GeV/c^2 , if the LSP mass is below 35 GeV/c^2 .

In the search for smuon production 5 events were selected, in agreement with the expected number from standard model processes. A mass limit for $\tilde{\mu}_R$ can be set at 70.3 GeV/c^2 if the LSP mass is below 35 GeV/c^2 .

The search for staus gave 7 candidates compatible with the expected background. A mass limit of 61.9 GeV/c^2 can therefore be set for the $\tilde{\tau}_R$ if the the mass difference between the stau and the LSP is above 15 GeV/c^2 . A mass limit of 59.9 GeV/c^2 can be set for the stau at minimum cross-section, under the same condition.

The search for stop and sbottom quarks, decaying into $c\tilde{\chi}^0_1$ and $b\tilde{\chi}^0_1$, respectively, gave 3 candidates well compatible with the expected background. For the stop, a mass limit of 68.5 GeV/c^2 is obtained for the state with minimal cross-section, if the mass difference between the squark and the LSP is above 15 GeV/c^2 . A mass limit of 43.6 GeV/c^2 is obtained for the sbottom quark under the same condition.

In the search for stop quarks decays into $b\ell\tilde{\nu}$, a mass limit of 73.2 GeV/c^2 can be obtained for the state with minimal cross-section, if the mass difference between the stop and the sneutrino is above 15 GeV/c^2 . A mass limit of 70.7 GeV/c^2 can be obtained under the same conditions when the stop decays into $b\tau\tilde{\nu}$.

These results extend substantially exclusion limits obtained at LEP1 and at LEP2 centre-of-mass energies of 130–172 GeV.

Acknowledgements

We express our gratitude to the members of the CERN accelerator divisions and compliment them on the fast and efficient commissioning and operation of the LEP accelerator in this new energy regime.

References

[1] DELPHI Collaboration: P. Abreu *et al.*, *Search for Scalar Fermions and Long-Lived Scalar Leptons at Centre-of-mass Energies of 130* GeV *to 172* GeV, submitted to E. Phys. J. C.

[2] ALEPH Collaboration: R. Barate *et al.*, *Search for sleptons in* e^+e^- *collisions at centre-of-mass energies up to 184 GeV*, CERN EP/98-077;
ALEPH Collaboration: R. Barate *et al.*, *Scalar quark searches at* $\sqrt{s}$ *= 181 – 184 GeV*, CERN EP/98-076;
L3 Collaboration: M. Acciarri *et al.*, *Search for Scalar Leptons, Charginos and Neutralinos in* e^+e^- *collisions at* $\sqrt{s}$ *= 161 – 172* GeV, CERN PPE/97-130, acc. by. E. Phys. J. C;
OPAL Collaboration: K. Ackerstaff *et al.*, Phys. Lett. **B396** (1997) 301;
OPAL Collaboration: K. Ackerstaff *et al.*, Z. Phys. **C75** (1997) 409.

[3] P. Fayet and S. Ferrara, Phys. Rep. **32** (1977) 249;
H.P. Nilles, Phys. Rep. **110** (1984) 1;
H.E. Haber and G. L.Kane, Phys. Rep. **117** (1985) 75.

[4] ALEPH Collaboration: R. Barate *et al.*, E. Phys. J. **C2** (1998) 417;
DELPHI Collaboration: P. Abreu *et al.*, E. Phys. J. **C1** (1998) 1;
L3 Collaboration: M. Acciarri *et al.*, op. cit., CERN PPE/97-130;
OPAL Collaboration: K. Ackerstaff *et al.*, E. Phys. J. **C2** (1998) 213.

[5] DELPHI Collaboration: P. Abreu *et al.*, Nucl. Instr. and Meth. **A303** (1991) 233.

[6] DELPHI Collaboration: P. Abreu *et al.*, Nucl. Instr. and Meth. **A378** (1996) 57.

[7] P. Rebecchi, "*Optimisation de l'herméticité du détecteur DELPHI pour la recherche de particules supersymétriques à LEP2* ", Ph.D.thesis, LAL 96-30, Université Paris XI Orsay.

[8] G. Borisov, C. Mariotti, *Performance of b-tagging in DELPHI at LEP2*, DAPNIA/Spp Report 97-06 and INFN/ISS Report 97-03;
G. Borisov, *Combined b-tagging*, DELPHI 97-94 PHYS 716,

[9] T. Sjöstrand, Comp. Phys. Comm. **82** (1994) 74;
T. Sjöstrand, "*High energy physics event generation with* `PYTHIA 5.7` *and* `JETSET 7.4`", CERN TH/7111-93 (1993, rev. 1994).

[10] DELPHI Collaboration: P. Abreu *et al.*, Z. Phys. **C73** (1996) 11.

[11] S.Katsanevas and S.Melachroinos in *Physics at LEP2*, CERN 96-01, Vol.2, p.328.

[12] S. Ambrosanio and B. Mele, Phys. Rev. **D52** (1995) 3900;
S. Ambrosanio and B. Mele, Phys. Rev. **D53** (1996) 2451.

[13] S. Kawabata, Comp. Phys. Comm. **41** (1986) 127.

[14] W. Beenakker, R. Hopker, M. Spira, and P.M. Zerwas, Phys. Lett. **B349** (1995) 463.

[15] F.A. Berends, R. Pittau, R. Kleiss, Comp. Phys. Comm. **85** (1995) 437.

[16] S. Nova, A. Olshevski, and T. Todorov, "*A Monte Carlo event generator for two photon physics*", DELPHI note 90-35 PROG 152.

[17] F.A. Berends, P.H. Daverveldt, R. Kleiss, Monte Carlo Simulation of Two-Photon Processes, Comp. Phys. Comm. 40 (86) 271-284.

[18] `DELSIM` *Reference Manual*, DELPHI note 87-97 PROG 100.

[19] A. Read, *Optimal statistical analysis of search results based on the likelihood ratio and and its application to the search for the MSM Higgs boson at 161 and 172* GeV, DELPHI note 97-158 PHYS 737.

[20] DELPHI Collaboration: P. Abreu *et al.*., Phys. Lett. **B372** (1998) 172.

[21] K. Mönig, *Model independent limit of the Z-decays Width into Unknown particles*, DELPHI note 97-174 PHYS 748.

[22] R.A. Fisher, *The use of multiple measurements in taxonomic problems*, Annals of Eugenics, **7** (1936).

[23] OPAL Collaboration: R. Akers *et al.*, Phys. Lett. **B337** (1994) 207.

[24] D0 Collaboration: S. Abachi *et al.*, Phys. Rev. Lett. **76** (1996) 2222.

[25] J. Ellis *et al.*, Phys. Lett. **B388** (1999) 97.

Observed events	11
Total background	12.7 ± 0.8
Bhabha events	1.5 ± 0.2
$Z^0/\gamma \to (\mu\mu, \tau\tau)(n\gamma)$	0.2 ± 0.1
4-fermions events	10.5 ± 0.8
$\gamma\gamma \to$ee, $\mu\mu, \tau\tau$	0.5 ± 0.1

Table 1: Selectron candidates, together with the total number of background events expected and the contributions from major background sources.

Observed events	5
Total background	6.1 ± 0.6
$Z^0/\gamma \to (\mu\mu$,ee, $\tau\tau)(n\gamma)$	0.2 ± 0.1
4-fermion events	5.8 ± 0.6
$\gamma\gamma \to$ee, $\mu\mu, \tau\tau$	0.1 ± 0.1

Table 2: Smuon candidates, together with the total number of background events expected and the contributions from major background sources.

Observed events	7
Total background	7.47 ± 0.60
$Z^0/\gamma \to (\mu\mu$,ee, $\tau\tau)(n\gamma)$	0.99 ± 0.30
4-fermion events	5.01 ± 0.31
$\gamma\gamma \to \tau^+\tau^-$	0.91 ± 0.21
$\gamma\gamma \to$ee, $\mu\mu$	0.56 ± 0.13

Table 3: Stau candidates for the selection in the mass region above 26.5 GeV/c^2, together with the total number of background events expected and the contributions from major background sources.

	$\Delta M > 10$ GeV/c^2		$\Delta M \leq 10$ GeV/c^2		
	1st DLA	2nd DLA	DLA ($\tilde{\mathrm{t}}$)	DLA ($\tilde{\mathrm{b}}$)	
E_{vis}	-0.068	-	-0.167	-	GeV
E_{30}	0.777	-	-	-	GeV
E^{ch}	-	-	-0.085	-	GeV
E (jet 1)	-	-0.021	-	-	GeV
E^{ch} (jet 1)	-	-	0.193	-	GeV
E_T (jet 1)	0.054	-	-	-	GeV
E_T (jet 2)	-	-	0.135	-	GeV
E_T^{ch} (jet 2)	-0.017	-	-	-	GeV
P_T^{miss}	-	-	0.203	-	GeV/c
M_{vis}	0.053	-	-	-	GeV/c^2
M_{recoil}	-	0.0002	-	-	GeV/c^2
$H_1 + H_3$	-	5.910	-	-	
$\cos(\phi_{acop})$	0.941	-	1.019	-	
ϕ_{acop}^{thr}	0.014	-	-	0.053	degree
ϕ_{acol}^{thr}	-	-	-	-0.036	degree
$\mathcal{P}_E^+$	-0.516	-	-0.672	-	
$\mathcal{P}_{comb}$	-	-	-	0.743	
θ_{iso}^{ch}	-0.004	-	-	-	degree
$\theta_{jet1,jet2}$	-0.081	-	-	-	degree
$\lvert\cos(\theta_{thr})\rvert$	-	-	-0.797	-3.480	

Table 4: Coefficients of the discriminating linear functions (DLA) used in the second step of the search for two-body decays of stop and sbottom. For the non-degenerate mass case the first and second functions applied to both the $\tilde{\mathrm{t}}$ and $\tilde{\mathrm{b}}$ selections (see text). Jets are ordered according to their energy. E_{vis} denotes the visible energy, E_{30} the energy in the polar angle interval $[30^\circ, 150^\circ]$, p_T^{miss} the missing transverse momentum, M_{vis} the visible mass, M_{recoil} the recoiling mass and H_i the i^{th} Fox-Wolfram moment. The superscript "ch" indicates use of charged tracks only and the subscript "T" quantities calculated in the transverse plane. $\mathcal{P}_E^+$ and $\mathcal{P}_{comb}$ are b-tagging probabilities as explained in the text. ϕ_{acop}^{thr} and ϕ_{acol}^{thr} denote acoplanarity and acollinearity with the two hemispheres being defined by the thrust axis. θ_{iso}^{ch} is the isolation angle of the most isolated charged particle, $\theta_{jet1,jet2}$ the angle between the two jets in their centre-of-mass system and θ_{thr} the polar angle of the thrust axis.

Selection	$\tilde{\mathrm{t}}$ and $\tilde{\mathrm{b}}$: $\Delta M > 10$ GeV/c^2				
	Data	MC	$Z^0(\gamma)$	4-f and Bhabha	$\gamma\gamma$
1st and 2nd step	2820	2697±18	2187	250	260
3rd step	26	27±3	5.4	7	14.5
$P_T^{miss} \geq 12$ GeV/c	20	17±2	4	7	5.6
$E(\mathrm{jet1}) \leq 60$ GeV $(E_{em}/E(\mathrm{jet1})) \leq 0.6$	8	5.0 ±0.7	1.2	4.8	0
$20^\circ \leq \theta_{jet} \leq 160^\circ$	5	4.2±0.4	0.9	3.3	0
$p_{iso} \leq 20$ GeV/c	4	3.2±0.4	0.9	2.3	0
$\lvert\cos(\theta_{thr})\rvert \leq 0.9$	3	2.8±0.3	0.5	2.3	0
$E_T^{ch}(\mathrm{jet2}) \geq 2$ GeV	1	2.4±0.3	0.2	2.2	0
$M_{vis} \leq 70$ GeV/c^2	1	2.1±0.3	0.18	1.92	0
$\langle E_{track}^{ch} \rangle \leq 4$ GeV	1	1.7±0.2	0.19	1.52	0

Table 5: Fourth step of the event selection for two-body decays of stop and sbottom in the non-degenerate mass case. E_{em} denotes the total electromagnetic energy, θ_{jet} the polar angles of any of the two jets and $\langle E_{track}^{ch} \rangle$ the average energy of a charged particle. For the other variables see Table 4.

Selection	$\tilde{\mathrm{t}}$: $\Delta M \leq 10$ GeV/c^2				
	Data	MC	$Z(\gamma)$	4f and Bhabha	$\gamma\gamma$
1st and 2nd step	565	532±8	142	33	349
3rd step	42	44±2	9.8	11.8	22.4
oblateness $\geq$0.1	38	37±2	9.1	10.4	18.5
$E_{30} \geq 0.9$ GeV	24	25±2	4.6	7.8	12.5
$E_{20} \geq 0.985$ GeV	20	22±1	3.8	7.1	11.0
$P_{tt} \leq 30$ GeV/c	8	13.0±1.3	0.19	1.8	11.0
$\phi_{acop}^{thr} \geq 20^\circ$	1	2.6±0.5	0.09	0.5	2.0
$\cos(\phi_{acop}) \geq -0.85$	1	0.97±0.23	0	0.29	0.68

Table 6: Fourth step of the event selection for two-body decays of stop squarks in the degenerate mass case. E_{20} (E_{30}) denote the fractions of the total energy for angles $> 20^\circ$ ($> 30^\circ$) from the beam axis. For the other variables see the text and Table 4.

Selection	$\tilde{b}$: $\Delta M \leq 10$ GeV/c^2				
	Data	MC	$Z(\gamma)$	4-f and Bhabha	$\gamma\gamma$
1st and 2nd step	729	629±8	101	46	583
3rd step	67	52±2	11	8	33
$E_{vis} \leq 40$ GeV	39	34±2	0.1	2	32
E_T^{ch}(jet1) ≥ 2 GeV	30	27±2	0.1	2	24.8
$20^\circ \leq \theta_{jets} \leq 160^\circ$	24	25±2	0.09	1	23.9
E_T (jet1) ≥ 5 GeV	8	14±1	0.09	0.5	13.4
$\phi_{acop}^{thr} \geq 20^\circ$	1	3±0.6	0.05	0.4	2.6
E_T^{ch}(jet2) ≥ 1 GeV	1	2.5±0.5	0.05	0.25	2.2
E_T (jet2) ≥ 2 GeV	1	1.6±0.4	0.05	0.15	1.38
oblateness ≤ 0.36	1	1.1±0.3	0.05	0	1.08

Table 7: Fourth step of the event selection for two-body sbottom decays in the degenerate mass case. The variables are explained in the caption of Table 4.

Squark	Data	MC
$\tilde{t}$	2	2.6±0.3
$\tilde{b}$	2	2.8±0.4

Table 8: Number of candidates and expected background in the search for two-body decays of stop and sbottom. Note that there is a substantial overlap between the two searches: they share one candidate and 2.0 expected background events.

	data	total background	$q\bar{q}$ (γ)	$\ell^+\ell^-$ (γ)	4-ferm	$\gamma\gamma$ (had)
preselection	3212	3193	1984.2	17.32	706.4	481.5
final selection	3	3.4	0.4	0.0	0.6	2.3

Table 9: Search for $\tilde{t} \to b\ell\tilde{\nu}$: number of events in data and background simulation after the first and second step of the selection, together with the background composition.

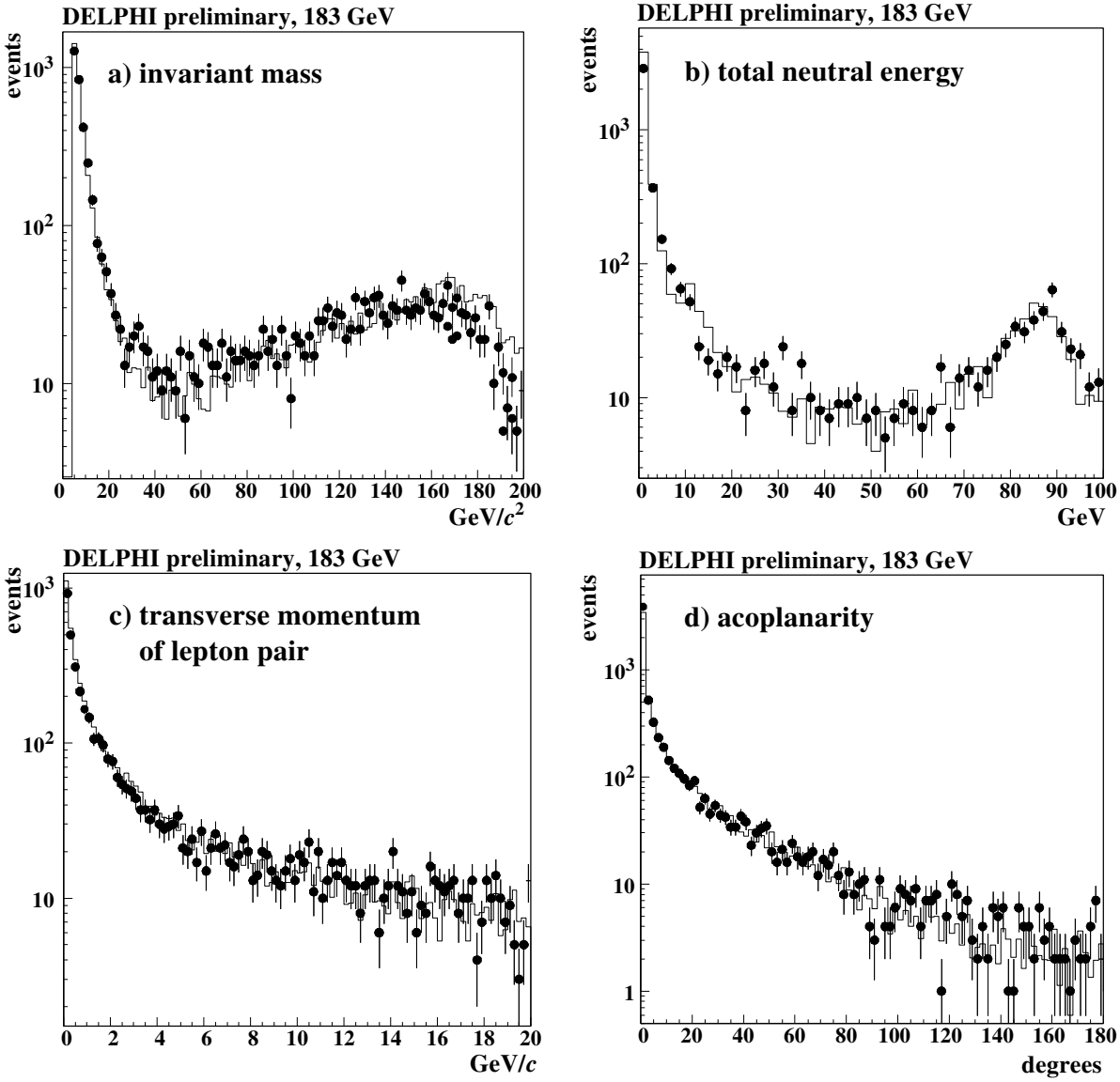

Figure 1: A comparison of data and background simulation in the selectron and smuon analysis after pre-selection of events with a pair of charged tracks. The dots with error bars represent the data while the simulation is shown by the solid line.

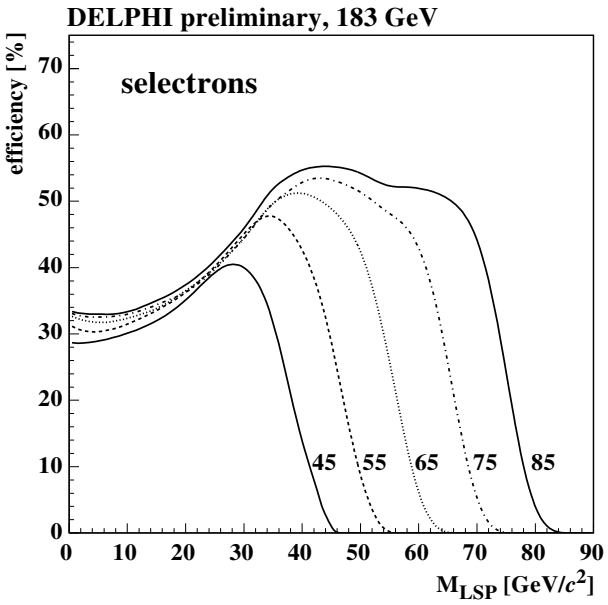

Figure 2: Efficiencies for the selectron selection. The curves correspond to different values of the selectron mass, which are indicated on the plot in units of GeV/c^2.

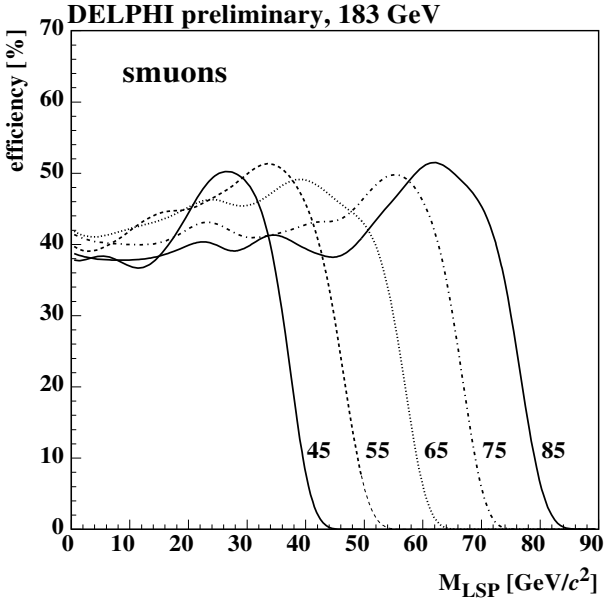

Figure 3: Efficiencies for the smuon selection. The curves correspond to different values of the smuon mass, which are indicated on the plot in units of GeV/c^2.

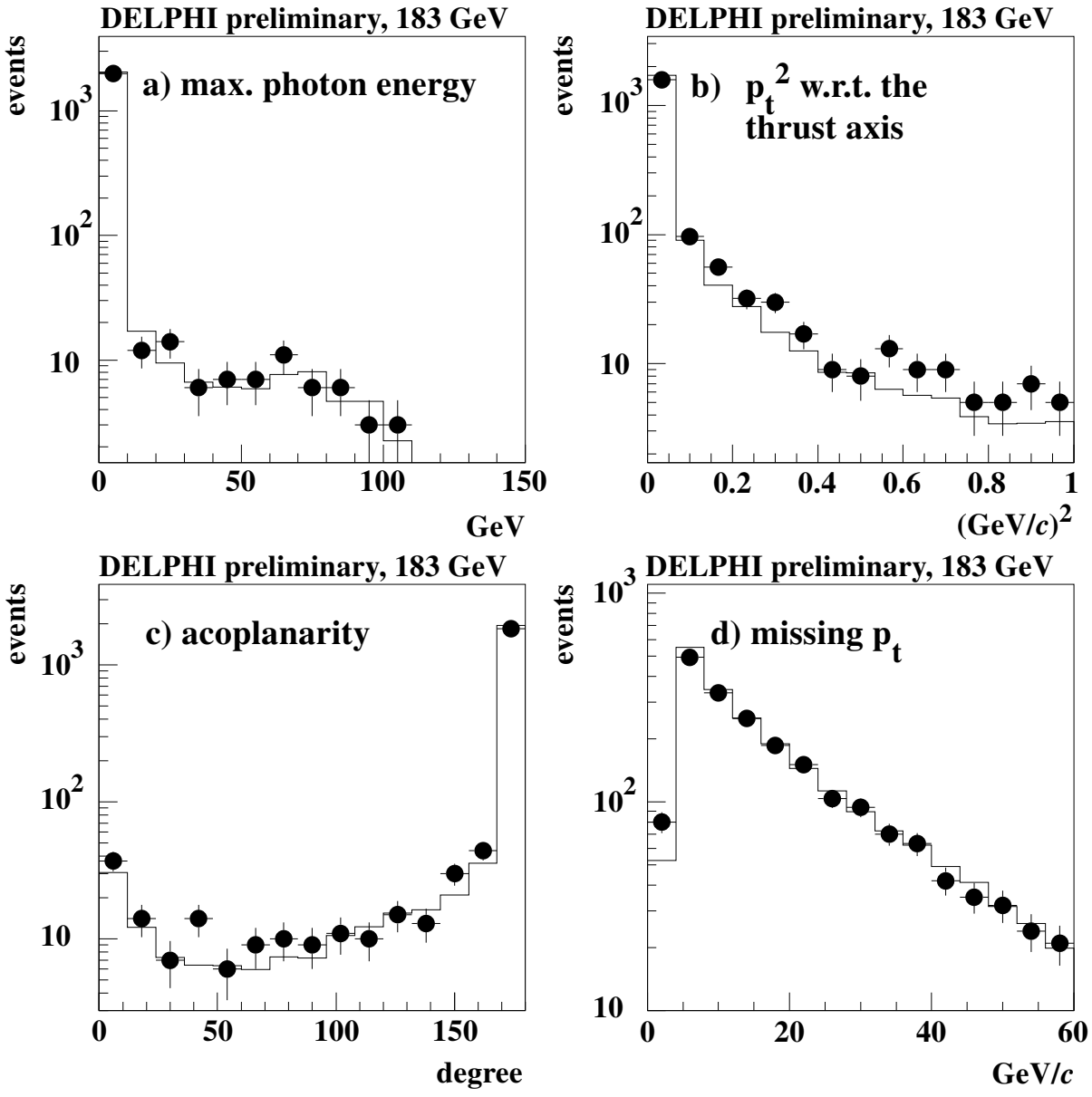

Figure 4: A comparison of data and simulation in the stau analysis for all events after selection of two groups of particles: (a) maximum photon energy, (b) transverse momentum of the particles with respect to the thrust axis, (c) acoplanarity and (d) missing transverse momentum. The dots with error bars represent the data while the simulation is shown by the solid line.

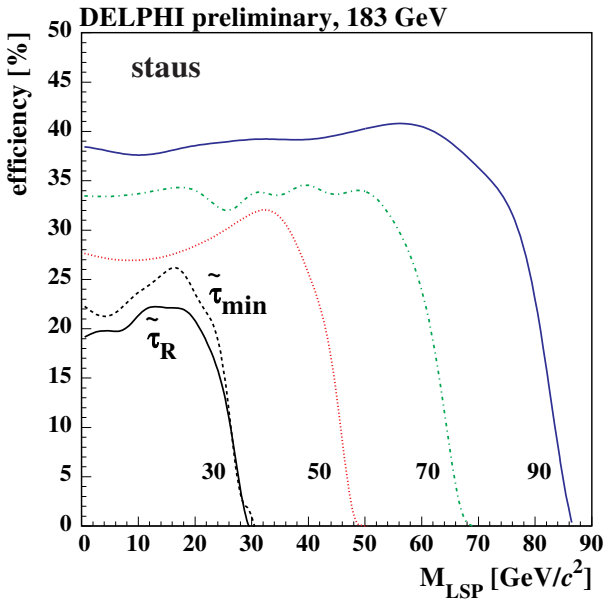

Figure 5: Efficiencies of the stau selection as a function of the LSP mass. The curves correspond to different stau masses, which are indicated on the plot in units of GeV/c^2. For stau masses below $M_Z/2$ the efficiencies depend on the coupling to the Z^0 and therefore on the mixing angle: The solid curve for $M_{\tilde{\tau}} = 30$ GeV corresponds to a mixing angle of 90°, whereas the dashed curve is valid for the $\tilde{\tau}$ state with minimum cross section. The statistical error is about 0.9% at 40% efficiency.

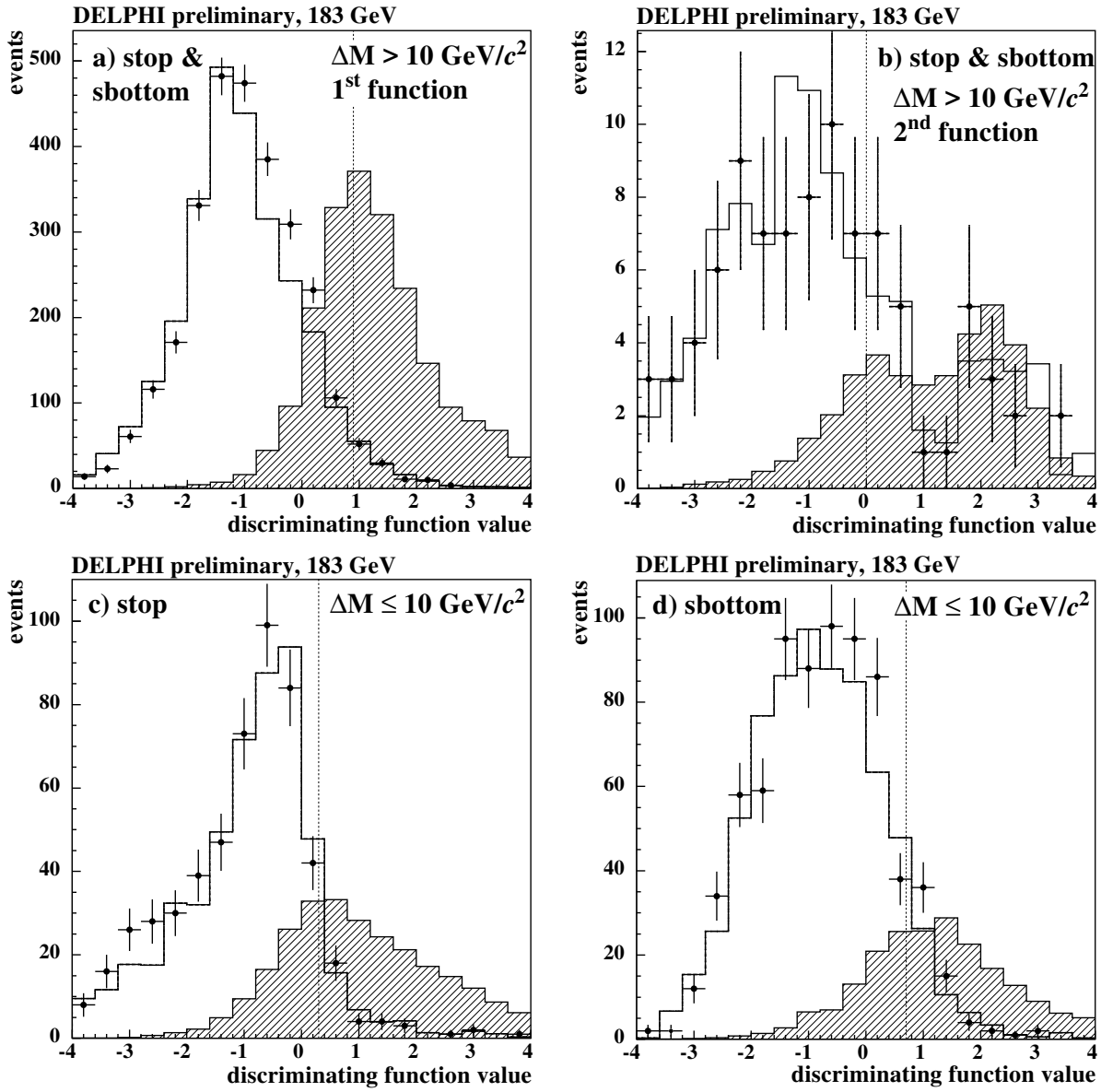

Figure 6: Discriminating functions used in the search for two-body decays of stop and sbottom: 1st and 2nd function used in the non-degenerate mass case for both $\tilde{t}$ and $\tilde{b}$ (a,b) and the functions for $\tilde{t}$ (c) and $\tilde{b}$ (d) with $\Delta M \leq 10\text{GeV}/c^2$. The points show the distribution from data and the histograms correspond to the expectation from background processes. The hatched histograms show all simulated signal samples. The dashed vertical lines indicate the cuts used in the selection. The cuts were set in order to reduce the Z(γ) background by a factor of 100 (a), the WW background by a factor of 10 (b). For the degenerate case the cuts were set in order to keep an efficiency of 25% (stop) and 10% (sbottom) for the mass point (80 GeV/c^2,75 GeV/c^2).

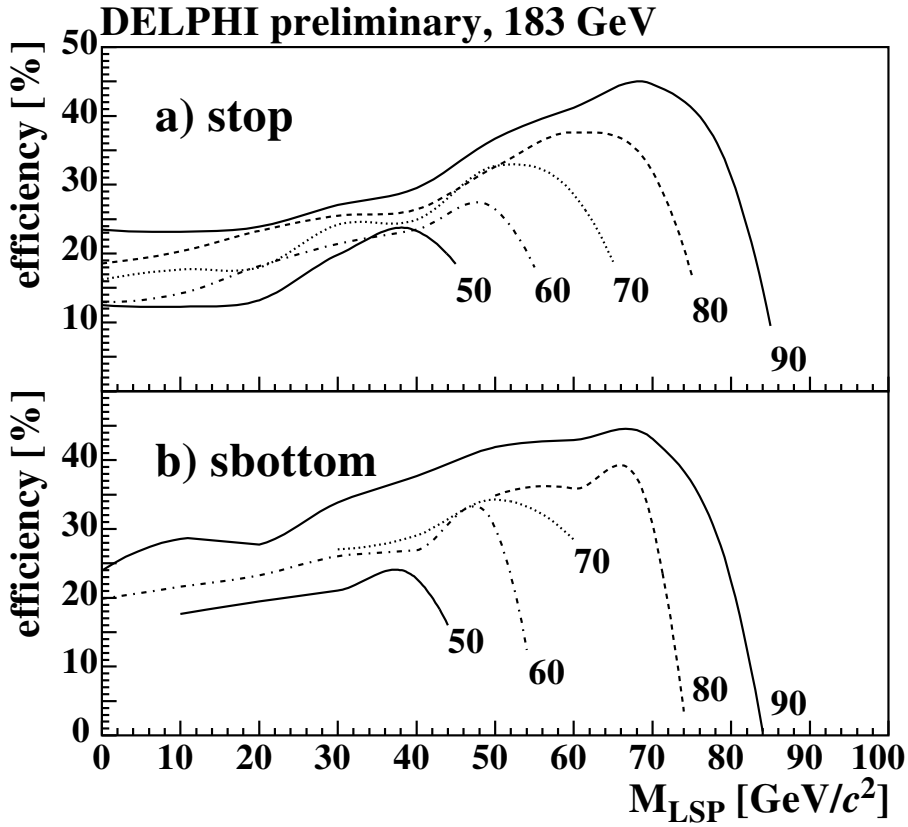

Figure 7: Efficiencies for the stop (top) and sbottom (bottom) selection in the search for two-body decays. The curves were determined by interpolation using 35 simulated samples in the (squark,neutralino) mass plane. They correspond to different values of the squark mass, which are indicated on the plots in units of GeV/c^2. The total uncertainty in the determination of the efficiency was about 10% relative for $\Delta M \leq 10$ GeV/c^2 and 15% for $\Delta M > 10$ GeV/c^2.

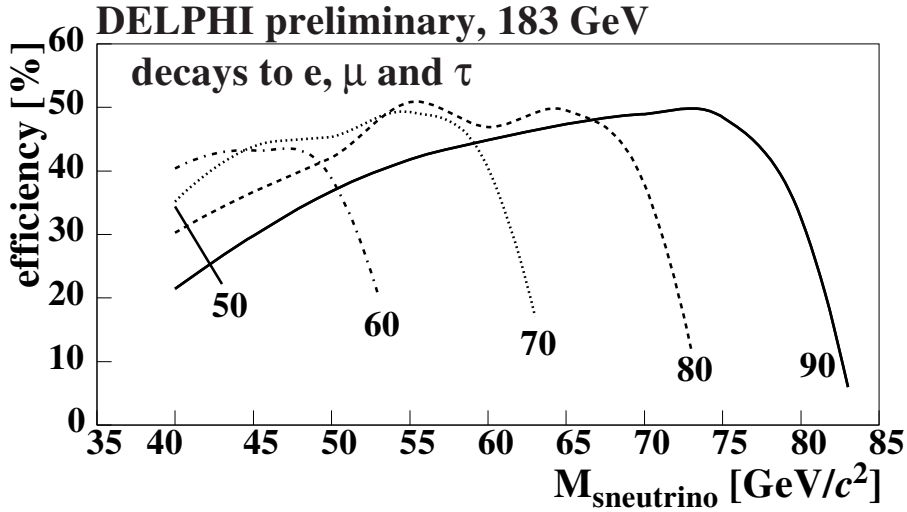

Figure 8: Selection efficiencies for stop decays into $b\ell\tilde{\nu}$, assuming equal branching fractions for electrons, muons and staus. The efficiencies are shown as a function of the sneutrino mass for different values of the stop mass (indicated in units of GeV/c^2).

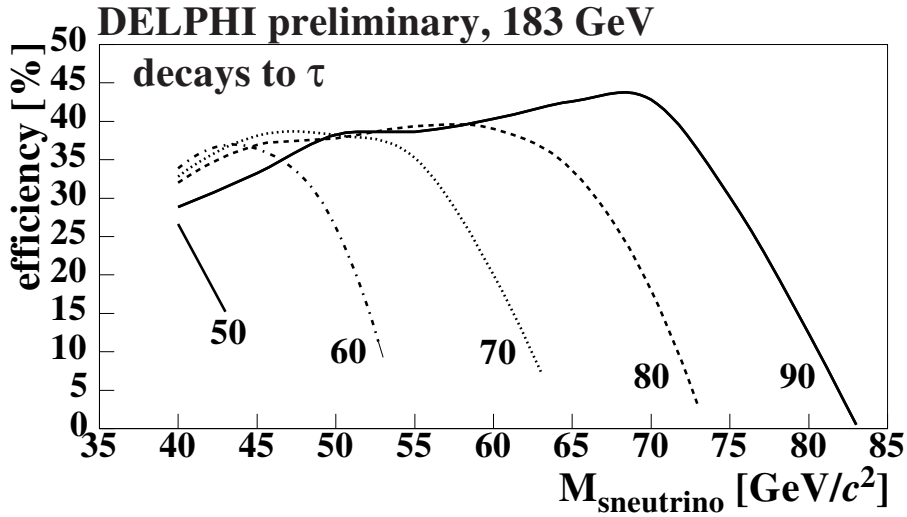

Figure 9: Selection efficiencies for stop decays into $b\tau\tilde{\nu}$ as a function of the sneutrino mass. The different curves correspond to different stop masses, which are indicated on the plot in units of GeV/c^2.

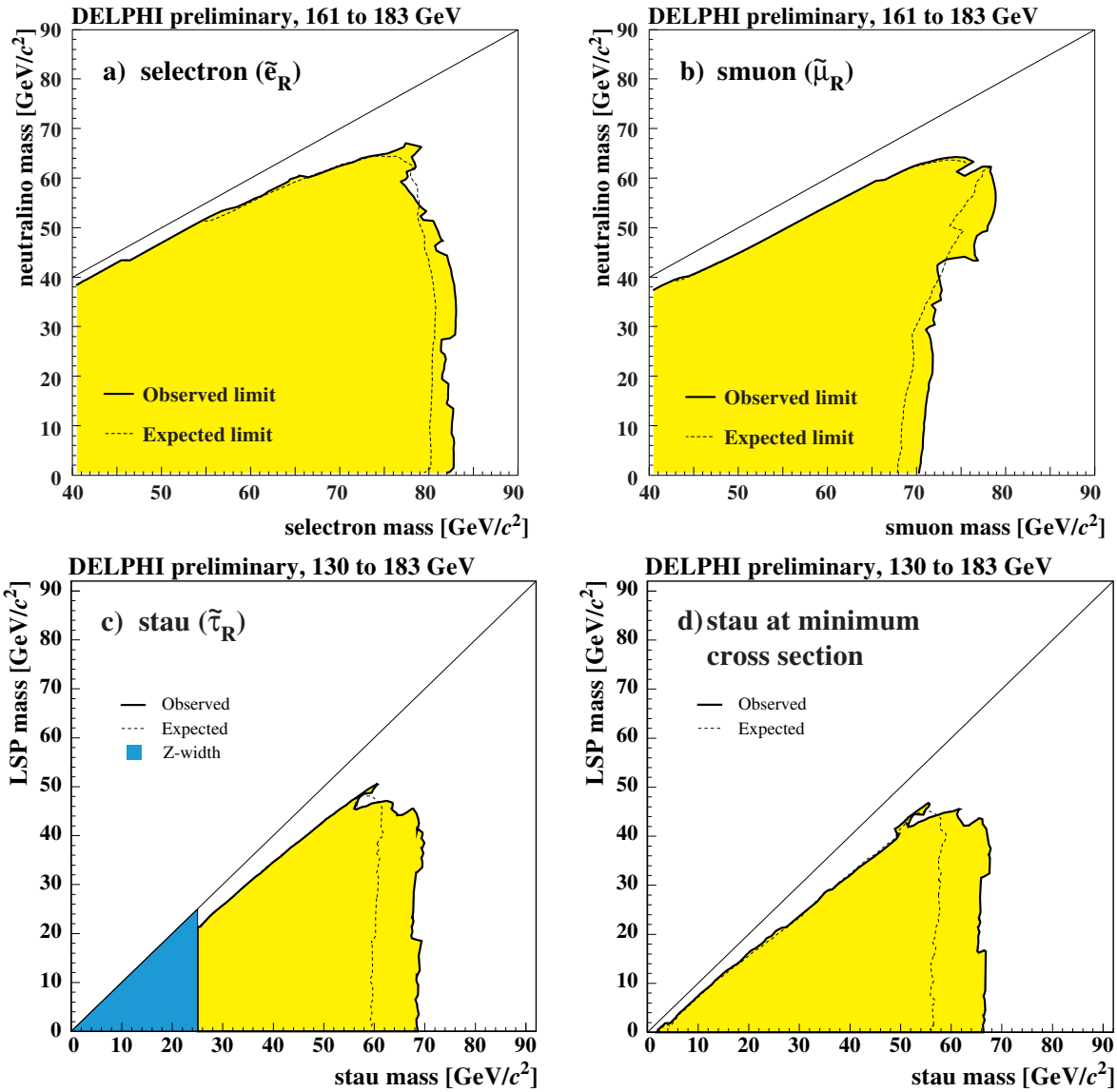

Figure 10: 95% confidence level exclusion regions for (a) right-handed selectrons ($\tilde{e}_R$) for $\mu = -100$, and $\tan\beta = 1.5$ (b) right-handed smuons ($\tilde{\mu}_R$) (c) right-handed staus ($\tilde{\tau}_R$) and (d) the stau state with minimum cross-section The dotted curves indicate the mean limit expected from background-only experiments.

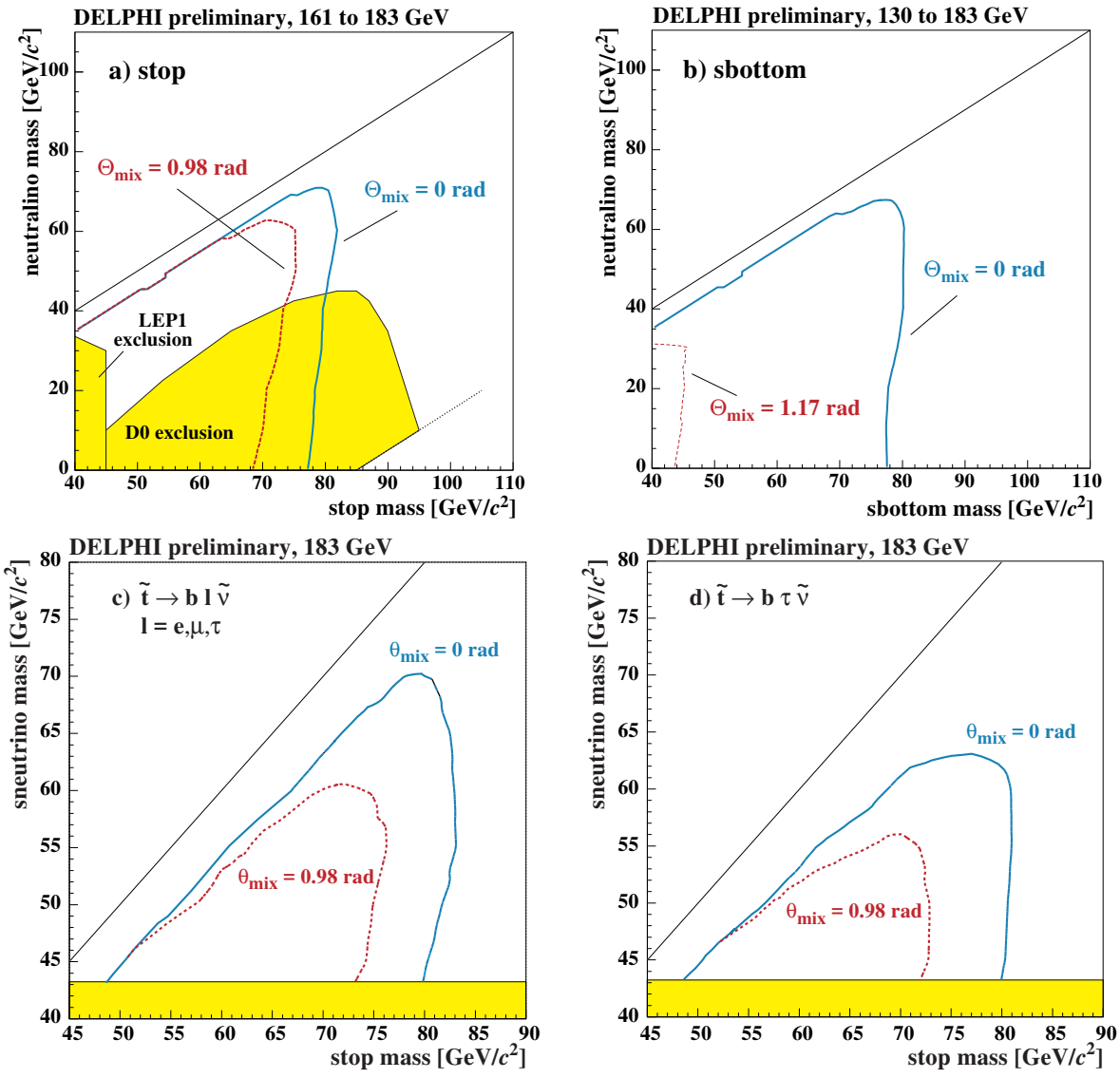

Figure 11: Exclusion domains at 95% confidence level. The solid curve correspond to a pure left-handed state ($\theta = 0$ rad) and dashed curve to the state with minimum cross section. (a) stop squark in the ($\tilde{t}$, $\tilde{\chi}^0_1$) mass plane, assuming 100% branching ratio into $c\tilde{\chi}^0_1$. The limits were obtained combining data at $\sqrt{s}$ = 161, 172 and 183 GeV. The shaded areas have been excluded by LEP1 [23] and D0 [24]. (b) sbottom quark in the ($\tilde{t}$, $\tilde{\chi}^0_1$) mass plane, assuming 100% branching ratio into $b\tilde{\chi}^0_1$. The limits were obtained combining data at $\sqrt{s}$ = 130 – 183 GeV. (c) stop quarks into $b\ell\tilde{\nu}$, in the ($\tilde{t}$,$\tilde{\nu}$) mass plane, assuming equal branching fractions into electrons, muons and staus. The shaded region indicates the current limit on the sneutrino mass [25]. (d) stop quarks, in the ($\tilde{t}$,$\tilde{\nu}$) mass plane, assuming 100% branching ratio into $b\tau\tilde{\nu}$. The shaded region indicates the current limit on the sneutrino mass.